Soft collisions in relativistic runaway electron avalanches

2010 J. Phys. D: Appl. Phys. 43 315206

(http://iopscience.iop.org/0022-3727/43/31/315206)

IOP PUBLISHING JOURNAL OF PHYSICS D: APPLIED PHYSICS

J. Phys. D: Appl. Phys. **43** (2010) 315206 (6pp) doi:10.1088/0022-3727/43/31/315206

Soft collisions in relativistic runaway electron avalanches

Sebastien Celestin and Victor P Pasko

CSSL, Penn State University, University Park, PA, USA

E-mail: sebastien.celestin@psu.edu

Received 9 March 2010, in final form 4 June 2010
Published 23 July 2010
Online at stacks.iop.org/JPhysD/43/315206

Abstract

This paper reports the first application of the relativistic binary-encounter-Bethe (RBEB) electron impact ionization model for studies of relativistic runaway electron avalanches (RREA) phenomenon at different pressures in air, which is believed to be the root cause of the hard x-rays and terrestrial gamma-ray flashes observed in the Earth's atmosphere in association with lightning activity. The model allows robust and accurate description of ionization over a wide range of energies (from the ionization threshold to megaelectronvolts), that is especially important for studies of thermal runaway electrons. A direct comparison between RREA rates obtained using classic Møller and the new RBEB differential ionization cross sections demonstrates that the dipole interaction between primary electrons and K-shell electrons of oxygen and nitrogen has an impact on the rates for relatively low applied electric fields comparable to or higher than 20 kV cm^{-1} at ground pressure. Implications of non-similarity of the runaway process developing at different altitudes due to the Swann–Fermi density effect are discussed.

1. Introduction

The enhancement of electric fields around tips of streamers is one of the unique naturally occurring circumstances in which fields $\sim 10E_k$, where E_k is the conventional breakdown threshold field defined by the equality of the ionization and dissociative attachment coefficients in air, can be dynamically produced and sustained for relatively extended periods of time. The ability of these streamer tip fields to generate runaway electrons was identified and discussed in the literature over two decades (Babich (1982) and references therein), and a new insight on this phenomenon has been given by recent laboratory experiments (Dwyer *et al* 2008, Nguyen *et al* 2008, 2010, Rahman *et al* 2008). Moreover, it has been proposed that with total potential differences on the order of tens of megavolts available in streamer zones of lightning leaders, during a highly transient negative corona flash stage of the development of negative stepped leader, electrons with energies 2–8 keV ejected from streamer tips near the leader head can be further accelerated to energies of hundreds of kiloelectronvolts and possibly to several tens of megaelectronvolts, depending on the particular magnitude of the leader head potential (Moss *et al* 2006). It has been proposed that these energetic electrons may be responsible (through the *bremsstrahlung* process) for the generation of hard x-rays observed from ground and satellites (e.g. Carlson *et al* (2009), Cummer *et al* (2005), Dwyer *et al* (2005), Fishman *et al* (1994), Inan *et al* (1996), Moore *et al* (2001), Smith *et al* (2005) and references therein). The current theories of transient luminous events occurring above cloud tops and termed blue and gigantic jets generally favour a phenomenological link between jet discharges and streamer zones of lightning leaders (Krehbiel *et al* (2008) and references therein) and it has been suggested that the thermal runaway electron process operating in leaders may contribute to the production of terrestrial gamma-ray flashes from the jet discharges (Moss *et al* 2006). This mechanism has been further supported by recent analysis indicating that peak fields in these discharges derived from spectrophotometric measurements had been significantly underestimated (Celestin and Pasko 2010).

The need for an accurate description of the electron runaway phenomena in air involving electron energy distributions with low initial energy (~1 eV) for a broad range of applied electric fields and describing coupling between high and low energy electron processes over many decades of electron energy (from sub-electronvolts to several megaelectronvolts) is an important task of the current

research actively pursued by several research groups (e.g. Chanrion and Neubert (2008, 2010), Colman *et al* (2010)).

In the study of the creation of runaway electrons with energies higher than 1 keV, usually only hard collisions (free projectile electron and free target electron) are considered through the Møller cross section (e.g. Dwyer and Smith (2005), Roussel-Dupré *et al* (1994)). This assumption is accurate if the energy of the secondary electron is much higher than its binding energy with the nucleus. This paper represents the first application of the relativistic binary-encounter-Bethe (RBEB) model (Kim *et al* 2000), which provides a robust and accurate description of ionization over a wide range of energies (from the ionization threshold to megaelectronvolts), to studies of relativistic runaway electron avalanche (RREA) phenomena at different pressures in air. We demonstrate that soft ionizing collisions between electrons and molecules (when target electrons cannot be considered as free particles) play a direct role in the RREAs developing under applied fields above $\sim$20 kV cm^{-1} in air at ground pressure. We also discuss non-similarity of RREAs developing at different altitudes due to the Swann–Fermi density effect.

2. Model formulation

2.1. Relativistic binary-encounter-Bethe model

The RBEB model (Kim *et al* 2000) is the relativistic extension of the binary-encounter-Bethe (BEB) model developed by Kim and Rudd (1994). The BEB model, applied to neutral molecules by Hwang *et al* (1996), gives very good results at low energy and is used to compute molecular databases provided by the National Institute of Standards and Technology (http://physics.nist.gov/PhysRefData/Ionization/molTable.html). The RBEB model is based on the combination of the free–free Møller cross section and the leading dipole part of the relativistic Bethe cross section (e.g. Inokuti (1971)). It results in an analytical representation of singly differential ionization cross section, which continuously covers a range of energy from the ionization threshold to the megaelectronvolt range. This continuous coverage over broad energy range makes it of first interest for the simulation of RREA and thermal runaway processes. Moreover, the RBEB model does not need any adjustable parameters and has been shown to be in very good agreement with the experiments (e.g. Kim *et al* (2000), Santos *et al* (2003)). This model only requires the average orbital kinetic energy and the binding energy of the target electron. These quantities are readily available in the literature (e.g. Hwang *et al* (1996), Santos *et al* (2003)).

In this work, we have computed the singly differential ionization cross section for O_2 and N_2 from the RBEB model for each molecular orbital and we summed them in the proportion of air (20% O_2 and 80% N_2). As will be shown in section 4, the K-shells are of particular importance in the calculations of this work, and we emphasize that the RBEB model provides accurate results for K-shells of light atoms such as N and O (Santos *et al* 2003).

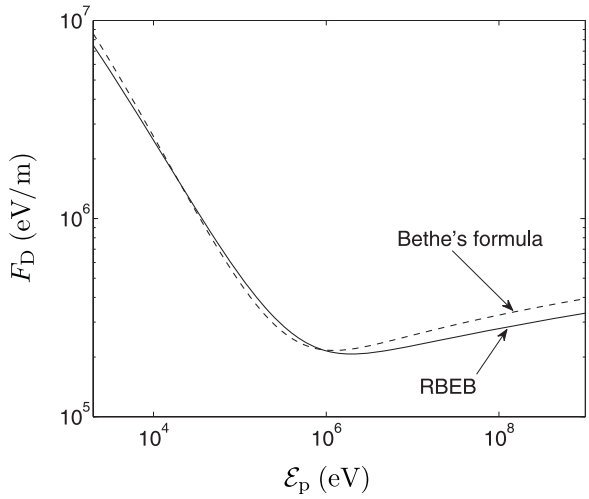

Figure 1. Comparison between the dynamic friction forces defined by the Bethe formula and computed using the RBEB model with respect to the energy.

2.2. Monte Carlo model

The Monte Carlo model developed in this work simulates the propagation and creation of electrons with kinetic energies between $\mathcal{E}_{min} = 2$ keV and 1 GeV, under the influence of constant applied electric field of magnitude E. The model closely follows the development presented by Lehtinen *et al* (1999). The present version of the model does not take into account ambient magnetic field. We consider homogeneous electric fields. The model is three-dimensional (3D) axisymmetric about the electric field in the momentum space and zero-dimensional (0D) in the configuration space.

While gaining energy from the electric field E, the electrons are losing energy from collisions with the molecules of the gas. The quantity associated with this process is the dynamic friction force F_D, which characterizes the average energy loss of an electron per unit of length. For energetic electrons, F_D can be defined by the Bethe formula (Bethe and Ashkin 1953, p 254, equation (52)), which takes into account hard (free-free) and soft (free-dipole) collisions. This function has a minimum at the electron kinetic energy $\mathcal{E} \simeq 1.2$ MeV (see figure 1). From this minimum we define the runaway threshold electric field $E_t/N \simeq 8$ Td (1 Td $= 10^{-21}$ V m^2), where N is the air density, above which an electron could gain more energy from the field than it loses due to collisions. Figure 1 shows F_D calculated using the RBEB model and the Bethe formula applied to air at atmospheric density at the ground level $N_0 = 2.688 \times 10^{25}$ m^{-3}. We see that both models give close results. In the Monte Carlo simulations presented below, we tested that the substitution of F_D given by RBEB with the Bethe formula does not lead to noticeable differences in results.

An electron gains energy through the relativistic equation of motion under the influence of the field E and is slowed down through F_D:

$$\frac{d\boldsymbol{p}}{dt} = q_e\boldsymbol{E} - F_D\frac{\boldsymbol{p}}{p}, \quad (1)$$

where $\boldsymbol{p} = \gamma m\boldsymbol{v}$ is the relativistic momentum, γ, m and $\boldsymbol{v}$ being respectively, the Lorentz factor, the mass and the velocity

of the electron, and q_e is the charge of the electron. The energy exchanges due to ionizing collisions creating secondary electrons with the energy $\mathcal{E}_s > \mathcal{E}_{min}$ are explicitly taken into account in our model. Therefore, the ionization processes leading to secondaries $\mathcal{E}_s > \mathcal{E}_{min}$ are subtracted from F_D before applying this force to the electrons (see Lehtinen *et al* 1999, equation (5)).

In the simulation, the time step is chosen so that one primary electron can hardly produce more than one secondary electron with an energy higher that 2 keV within one time step. However, during this time step, electrons experience a lot of elastic collisions. Therefore, the angular diffusion of electrons is mainly considered through the process of multiple scattering of electrons from elastic collisions. The method of computation is set as prescribed in Lehtinen *et al* (1999) by considering small angles of deviations $\Delta\Theta$ and the equation:

$$\frac{d\langle\Theta^2\rangle}{dt} = \frac{4\pi N Z_m^2 r_e^2 c^4}{v^3\gamma^2} \ln\left(\frac{164.7}{Z_m^{1/3}}\frac{p}{mc}\right), \quad (2)$$

where c is the speed of light in vacuum, r_e is the classical electron radius and $Z_m \simeq 14.5$ is the mean molecular charge for air. The momentum of the primary and secondary electrons after an ionizing collision is determined by the energy–momentum conservation law, that is the angles θ_p and θ_s between the momentum of the primary electron before collision and the primary and secondary electrons after ionizing collision, respectively, are defined by the formulae:

$$\cos\theta_p = \sqrt{\frac{(\mathcal{E}_p - \mathcal{E}_s)(\mathcal{E}_p + 2mc^2)}{\mathcal{E}_p(\mathcal{E}_p - \mathcal{E}_s + 2mc^2)}}, \quad (3)$$

$$\cos\theta_s = \sqrt{\frac{\mathcal{E}_s(\mathcal{E}_p + 2mc^2)}{\mathcal{E}_p(\mathcal{E}_s + 2mc^2)}}, \quad (4)$$

where $\mathcal{E}_p$ and $\mathcal{E}_s$ are the energy of primary and secondary electrons, respectively.

The simulation starts with 5000 electrons launched at 1 MeV in the antiparallel direction of the electric field. In order to keep track of primary and secondary electrons without increasing the computation times much, we have developed a 2-bins remapping technique (Kunhardt and Tzeng 1986, Moss *et al* 2006). This technique reduces the number of particles effectively taken into account in the computations by merging them into super-particles, such that each of the super-particles actually represents many particles. First, the energy spectrum of electrons is separated into two groups. Then, the remapping method is applied on the lowest energy group, such that the information on high-energy particles is not degraded (Moss *et al* 2006, section 2.6). A representation of the results given by such a method is illustrated in figure 3.

The probability of creation of a secondary electron having the kinetic energy $\mathcal{E}_s > \mathcal{E}_{min}$ by electron impact with a primary electron with energy $\mathcal{E}_p$ during the timestep Δt is given by $P(\mathcal{E}_p, \mathcal{E}_s > \mathcal{E}_{min}) = N v \Delta t \sigma(\mathcal{E}_p, \mathcal{E}_s > \mathcal{E}_{min})$ (Lehtinen *et al* 1999), where N is the gas density, v is the velocity of the primary electron and $\sigma(\mathcal{E}_p, \mathcal{E}_s > \mathcal{E}_{min})$ is the cross section of this event that is defined as

$$\sigma(\mathcal{E}_p, \mathcal{E}_s > \mathcal{E}_{min}) = \int_{\mathcal{E}_{min}}^{\mathcal{E}_p/2} \frac{d\sigma_{ion}}{d\mathcal{E}_s}(\mathcal{E}_p, \mathcal{E}_s)\, d\mathcal{E}_s, \quad (5)$$

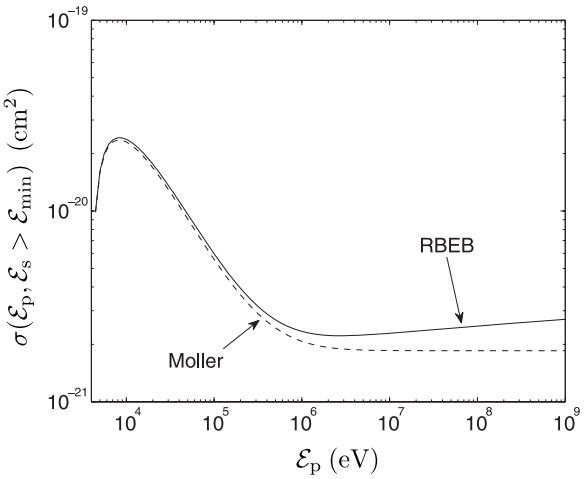

Figure 2. Comparison between cross sections of ionization leading to $\mathcal{E}_s > 2$ keV with respect to the energy of the primary electron using Møller and RBEB models in air. On this graph, the rise in the RBEB cross section above ∼1 MeV is due to the dipole interaction between the primary electron and the K-shell electrons.

Table 1. Values of the critical runaway energy $\mathcal{E}_{run}$ with respect to the applied electric field given by dynamic friction force functions using differential cross sections provided by Møller or RBEB models (see figure 1).

$\delta = E/E_t$	2	5	8	10	12	15
$\mathcal{E}_{run}$ (keV) Møller	549	103	54	41	32	24
$\mathcal{E}_{run}$ (keV) RBEB	583	112	57	42	33	24

where $d\sigma_{ion}/d\mathcal{E}_s$ is the singly differential cross section of ionization. In this work $\sigma(\mathcal{E}_p, \mathcal{E}_s > \mathcal{E}_{min})$ has been defined either by Møller differential cross section with a mean molecular charge $Z_m = 14.5$ or by the RBEB model applied to O_2 and N_2. The comparison of $\sigma(\mathcal{E}_p, \mathcal{E}_s > \mathcal{E}_{min})$ given by these models is shown in figure 2 (see section 4).

The energy of the secondary electron is determined through the generation of a random number R_s in the interval [0, 1] and the numerical inversion of the singly differential cross section given either by Møller or RBEB models (e.g. see Lehtinen *et al* (1999), equation (17)), that is by solving numerically the following equation for $\mathcal{E}_s$:

$$R_s = \frac{1}{\sigma(\mathcal{E}_p, \mathcal{E}_s > \mathcal{E}_{min})} \int_{\mathcal{E}_{min}}^{\mathcal{E}_s} \frac{d\sigma_{ion}}{d\mathcal{E}_s}(\mathcal{E}_p, \mathcal{E}_s)\, d\mathcal{E}_s. \quad (6)$$

The critical runaway energy $\mathcal{E}_{run}$ above which an electron is considered to be runaway is computed for each applied electric field studied by comparison between the applied electric field, the dynamic friction force, and the average cosine of angles between momentum of electrons and the direction of the applied electric field, as fully described in Lehtinen *et al* (1999). As shown in figure 1 the dynamic friction forces given by the Bethe formula and RBEB cross sections are in good agreement (see table 1), therefore the values of $\mathcal{E}_{run}$ given by both of these approaches give very close results. Indeed, the variations in values of $\mathcal{E}_{run}$ between the two models shown in table 1 do not lead to noticeable differences in the results of simulation.

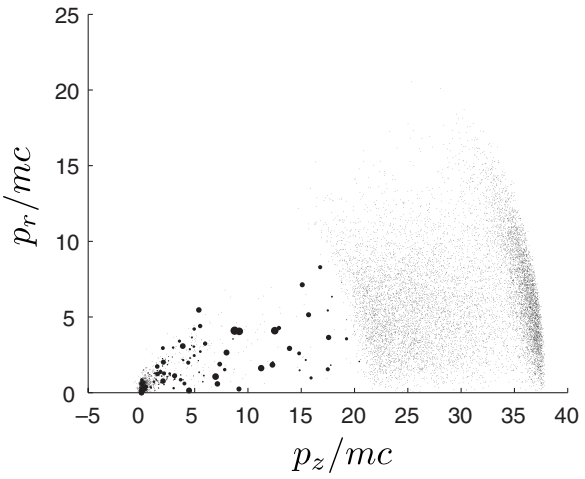

Figure 3. Electrons in the momentum space at $t = 64.6$ ns for an applied electric field with magnitude corresponding to $\delta = 5$. The area of points is proportional to the number of electrons that are actually represented by one super-particle.

The simulation of photons and positrons and therefore related feedback effects (e.g. Babich *et al* (2005), Dwyer (2003)) are not included in the present study.

3. Results

In the literature, results on RREA rates are often provided with respect to the relativistic runaway over-voltage $\delta = E/E_t = E(\mathrm{V\,m^{-1}})/215 \times 10^3$ at the ground level air density $N_0 = 2.688 \times 10^{25}\,\mathrm{m^{-3}}$, where E is the applied electric field (e.g. Babich *et al* (2001), Lehtinen *et al* (1999)). The computations have been realized for applied electric fields corresponding to $\delta = 2$, 5, 8, 10, 12, 15 and 20. For each applied electric field, we have launched 10 simulations during a time of 1 μs in order to accurately evaluate the statistical errors in the results, presented by the error bars in figure 5.

Figure 3 shows a representative distribution of electrons in the momentum space at $t = 64.6$ ns for an applied electric field with magnitude corresponding to $\delta = 5$. In this figure, super-particles are represented by points with areas proportional to the number of actual electrons they represent because of the remapping technique. As discussed above, since we want to keep a high resolution for the particles with the highest energies, we clearly see that only particles with lowest energies are affected by the remapping technique. The quantities p_z and p_r in figure 3 are the momentum components along and perpendicular to the direction of the electric field, respectively. Figure 3 also demonstrates the highly directional motion of electrons along the direction of the electric field.

From the results of the Monte Carlo simulations we can compute the electron energy distribution function (EEDF). As an example, figure 4 shows the EEDF normalized to 1 for energies higher than $\mathcal{E}_{\min} = 2$ keV, for an applied electric field corresponding to $\delta = 10$ and using the RBEB model for ionization. That is,

$$\int_{\mathcal{E}>2\,\mathrm{keV}} f(\mathcal{E})\,\mathrm{d}\mathcal{E} = 1, \tag{7}$$

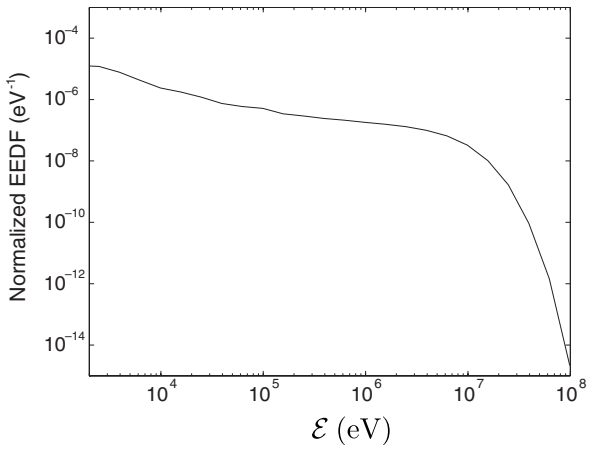

Figure 4. Electron energy distribution function (EEDF) normalized to 1 for energies higher than 2 keV. In this calculation $\delta = 10$ and the RBEB model was used for ionization. The EEDF has been averaged in time after convergence was obtained (between $t = 13$ and 167 ns).

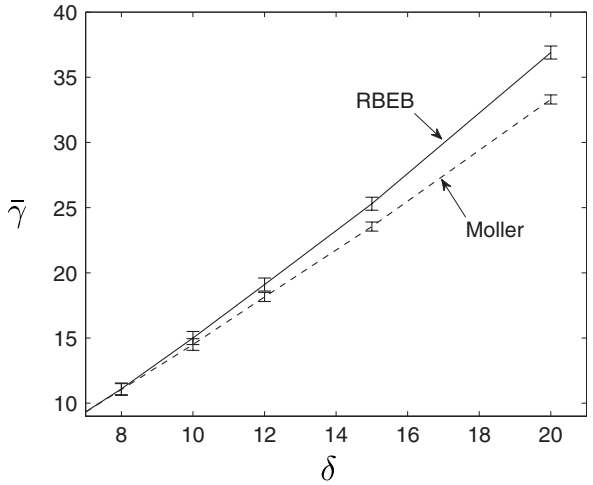

Figure 5. RREA rates presented in terms of $\bar{\gamma} = \gamma(\mathrm{ns^{-1}}) \times 171.53$ versus the relativistic runaway over-voltage $\delta = E(\mathrm{V\,m^{-1}})/215 \times 10^3$, for $\delta = 8$, 10, 12, 15 and 20. Rates for lower δ given by both models have been observed to be identical.

where $f(\mathcal{E})$ is the EEDF. The characteristic features of this distribution are in good agreement with distributions shown in Lehtinen *et al* (1999, Figure 5).

The number of runaway electrons N_{run} increases in time and can be fitted by the relation $N_{\mathrm{run}} = 5000\exp(\gamma t)$, where 5000 is the initial number of electrons and γ is the RREA rate. Figure 5 presents the RREA rates obtained in this study with respect to δ. In figure 5, rates are presented in terms of $\bar{\gamma} = \gamma\tau$, using $\tau = (2\pi N_0 14.5 r_e^2 c)^{-1} \simeq 171.53$ ns allowing for direct comparison with the results of Lehtinen *et al* (1999).

The RREA rates computed using the Møller cross section are in good agreement with those documented in Lehtinen *et al* (1999), which validates the numerical techniques employed in this work. These rates are also confirmed by other research groups (e.g. Babich *et al* (2001), Coleman and Dwyer (2006)).

The rates obtained using the RBEB model are similar at low electric field to those obtained with the Møller model. Indeed, the rates have been found to be identical between

$\delta = 2$ and 8. However, for electric fields corresponding to $\delta \gtrsim 10$, figure 5 presents a deviation from the results given by the use of Møller differential cross section. Quantitatively, for an electric field corresponding to $\delta = 15$ ($\sim E_k$) at $t = 1\,\mu$s (corresponding to a propagation distance of $\sim$300 m at the speed of light) the ratio between the number of runaway electrons obtained using the RBEB model and Møller cross section is $\sim 2.7 \times 10^4$. This number can be compared with the ratio between the number of runaway electrons obtained in the cases of upper and lower limits for one given model of cross section represented by error bars in figure 5, which is $\sim$340 in the RBEB case and $\sim$80 in the Møller case. We discuss this deviation in RREA rates in the next session.

4. Discussion

We have verified that the deviation obtained in RREA rates (figure 5) mainly comes from the discrepancies between cross sections shown in figure 2. In fact, the relative difference between the cross sections represented in figure 2 is as high as $\sim$15% for $\mathcal{E}_p \simeq 1$ MeV and $\sim$35% for $\mathcal{E}_p \simeq 100$ MeV. The increase in the cross section given by the RBEB model for $\mathcal{E}_p \gtrsim 1$ MeV is the high-energy part ($\mathcal{E}_s > 2$ keV) of an effect called the relativistic rise in cross sections and is due to the dipole interaction (e.g. Santos *et al* (2003)) taken into account in the RBEB model, and not included in the Møller cross section that only characterizes hard collisions (free electron colliding with a free electron at rest). The Møller cross section gives accurate results if $\mathcal{E}_s \gg B$, where B is the binding energy of the target electron. Increasing the applied electric fields results in decreasing $\mathcal{E}_{\rm run}$. For example, for $\delta = 15$ we find $\mathcal{E}_{\rm run} \simeq 24$ keV, whereas the binding energies of the K-shell electrons of O and N are $\sim$0.54 keV and $\sim$0.41 keV, respectively (e.g. Santos *et al* (2003)). Although the Møller cross section has been considered as sufficiently accurate, figure 5 shows that the dipole-type interaction plays a non-negligible role in the ionization process leading to secondary electrons created with energies of a few tens of kiloelectronvolts.

Indeed, artificially setting the binding energies of K-shell electrons to energies typical for L-shell electrons (tens of eVs) in the RBEB formulation makes the cross sections presented in figure 2 match, since in this case only hard collisions ($\mathcal{E}_s \gg B$) are taken into account, and thus RREA rates get very close to those computed using the Møller cross section.

The results presented in this paper on RREA rates have been obtained at the density of air at ground level $N_0 = 2.688 \times 10^{25}\,\mathrm{m}^{-3}$ and are scalable proportionally to the density of air allowing to find related rates for the same reduced electric fields E/N at any altitude of interest. The passage of high-energy electrons through a medium results in an effect of polarization of atoms known as the *Swann–Fermi density effect* (Fermi 1940), or simply *density effect*, which can be introduced directly in cross sections (e.g. ICRU Report 37 (1984), Scofield (1978)), and is related to the density of the gas. Thus, the density effect introduces a non-similarity between RREAs propagating at different altitudes. In order to present scalable results with altitude, we have not included the density effect in our calculations. From the values of the corrections due to the density effect presented in ICRU Report 37 (1984) one gets a reduction in the collisional dynamic friction force of 3.4% at 100 MeV and 11.8% at 1 GeV, in air at ground pressure. From ICRU Report 37 (1984, equation (6.3)) one can calculate that this effect would decrease to 9% at 10 km altitude, 5% at 20 km and become <1% above 30 km, for 1 GeV electrons.

In the existing literature (e.g. Babich *et al* (2004)) the effect of soft collisions with inner shell electrons on RREA rates was not discussed and quantified when the EEDL database, which takes K-shells into account (Cullen *et al* 1991), was used. Indeed, we have verified that the use of EEDL database in our code gives results very close to those obtained using Møller cross section, similarly to results reported by Babich *et al* (2004). Cullen *et al* (1991) have stated that the saturation of cross sections provided in the EEDL (no relativistic rise) is due to the density effect. Thus, the density effect compensates the effect of soft ionizing collisions with K-shell electrons on RREA rates at high air pressures. Assuming that the density effect is correctly calculated in the EEDL implies that the non-similarity of RREA at different altitudes due to this effect should be noticeable when ground rates are scaled to/compared with those at low air density at high altitudes (i.e. cloud tops).

5. Summary and concluding remarks

Principal results of this work can be summarized as follows:

(i) We have reported the first application of the RBEB model to studies of RREA phenomena in air. It is well known that Møller cross section cannot be used for ionization processes leading to low energy secondary electrons (see discussion in Roussel-Dupré *et al* (1994)). The RBEB model allows for computing accurate ionization cross sections seamlessly over a very wide range of energy (from ionization threshold to megaelectronvolts) for both primary and secondary electrons, that is especially important for studies of thermal electron runaway phenomena (e.g. Chanrion and Neubert (2010), Colman *et al* (2010)). Since the RBEB formulation is analytical, it is directly implementable in Boltzmann or Monte Carlo codes, and since it does not require any adjustable parameters it is straightforward to apply it for different gases, for example, in order to simulate relativistic breakdown in planetary atmospheres (e.g. Dwyer (2007), Roussel-Dupré *et al* (2008)).

(ii) A direct comparison of the RREA rates obtained using the Møller and RBEB differential ionization cross sections have shown that the dipole interaction between primary electrons and K-shells of N and O leading to the generation of energetic secondary electrons has an impact on RREA rates for applied electric fields higher than $\sim$20 kV cm^{-1}.

(iii) The Swann–Fermi density effect included in the database EEDL compensates the effect of soft ionizing collisions with K-shell electrons on RREA rates. Therefore, assuming that the density effect is correctly calculated in the EEDL implies that the RREAs developing at ground pressure are not directly scalable to those developing at

higher altitudes (i.e. cloud tops) where the density effect is negligible.

Acknowledgments

This research was supported by the NSF grants AGS-0734083 and AGS-0741589 to Penn State University.

References

Babich L P, Donskoy E N, Il'kaev R I, Kutsyk I M and Roussel-Dupré R A 2004 Fundamental parameters of a relativistic runaway electron avalanche in air *Plasma Phys. Rep.* **30** 616

Babich L P, Donskoy E N, Kutsyk I M and Roussel-Dupré R A 2005 The feedback mechanism of runaway air breakdown *Geophys. Res. Lett.* **32** L09809

Babich L P, Donskoy E N, Kutsyk I M, Kudryavtsev A Y, Roussel-Dupré R A, Shamraev B N and Symbalisty E M D 2001 Comparison of relativistic runaway electron avalanche rates obtained from Monte Carlo simulations and kinetic equation solution *IEEE Trans. Plasma Sci.* **29** 430

Babich L P 1982 A new type of ionization wave and the mechanism of polarizational self-acceleration of electrons in gas discharges at high overvoltages *Sov. Phys.—Dokl.* **263** 76

Bethe H A and Ashkin J 1953 *Experimental Nuclear Physics* vol I (New York/London: Wiley/Chapman and Hall)

Carlson B E, Lehtinen N G and Inan U S 2009 Terrestrial gamma ray flash production by lightning current pulses *J. Geophys. Res.* **114** A00E8

Celestin S and Pasko V P 2010 Effects of spatial non-uniformity of streamer discharges on spectroscopic diagnostics of peak electric fields in transient luminous events *Geophys. Res. Lett.* **37** L07804

Chanrion O and Neubert T 2008 A PIC-MCC code for simulation of streamer propagation in air *J. Comput. Phys.* **227** 7222

Chanrion O and Neubert T 2010 Production of runaway electrons by negative streamer discharges *J. Geophys. Res.* **115** A00E32

Coleman L M and Dwyer J R 2006 Propagation speed of runaway electron avalanches *Geophys. Res. Lett.* **33** L11810

Colman J J, Roussel-Dupré R A and Triplett L 2010 Temporally self-similar electron distribution functions in atmospheric breakdown: The thermal runaway regime *J. Geophys. Res.* **115** A00E16

Cullen D, Perkins S and Seltzer S 1991 Tables and graphs of electron interaction cross 10 eV to 100 GeV derived from the LLNL evaluated electron data library (EEDL), $Z = 1$–100 *Lawrence Livermore National Laboratory*

Cummer S A, Zhai Y, Hu W, Smith D M, Lopez L I and Stanley M A 2005 Measurements and implications of the relationship between lightning and terrestrial gamma ray flashes *Geophys. Res. Lett.* **32** L08811

Dwyer J R and Smith D M 2005 A comparison between Monte Carlo simulations of runaway breakdown and terrestrial gamma-ray flash observations *Geophys. Res. Lett.* **32** L22804

Dwyer J R *et al* 2005 X-ray bursts associated with leader steps in cloud-to-ground lightning *Geophys. Res. Lett.* **32** L01803

Dwyer J R, Saleh Z, Rassoul H K, Concha D, Rahman M, Cooray V, Jerauld J, Uman M A and Rakov V A 2008 A study of X-ray emission from laboratory sparks in air at atmospheric pressure *J. Geophys. Res.* **113** D23207

Dwyer J R 2003 A fundamental limit on electric fields in air *Geophys. Res. Lett.* **30** 2055

Dwyer J R 2007 Relativistic breakdown in planetary atmospheres *Phys. Plasmas* **14** 042901

Fermi E 1940 The ionization loss of energy in gases and in condensed materials *Phys. Rev.* **57** 485

Fishman G et al 1994 Discovery of intense gamma-ray flashes of atmospheric origin *Science* **264** 1313

Hwang W, Kim Y-K and Rudd M E 1996 New model for electron-impact ionization cross sections of molecules *J. Chem. Phys.* **104** 2956

ICRU Report 37 1984 Stopping powers for electrons and positrons, International Commision on Radiation Units and Measurements

Inan U S, Reising S C, Fishman G J and Horack J M 1996 On the association of terrestrial gamma-ray bursts with lightning and implications for sprites *Geophys. Res. Lett.* **23** 1017

Inokuti M 1971 Inelastic collisions of fast charged particles with atoms and molecules—the Bethe theory revisited *Rev. Mod. Phys.* **43** 297

Kim Y-K and Rudd M E 1994 Binary-encounter-dipole model for electron-impact ionization *Phys. Rev.* A **50** 3954

Kim Y-K, Santos J P and Parente F 2000 Extension of the binary-encounter-dipole model to relativistic incident electrons *Phys. Rev.* A **62** 052710

Krehbiel P R, Riousset J A, Pasko V P, Thomas R J, Rison W, Stanley M A and Edens H E 2008 Upward electrical discharges from thunderstorms *Nature Geosci.* **1** 233

Kunhardt E E and Tzeng Y 1986 Monte Carlo technique for simulating the evolution of an assembly of particles increasing in number *J. Comput. Phys.* **67** 279

Lehtinen N G, Bell T F and Inan U S 1999 Monte Carlo simulation of runaway MeV electron breakdown with application to red sprites and terrestrial gamma ray flashes *J. Geophys. Res.* **104** 24699

Moore C B, Eack K B, Aulich G D and Rison W 2001 Energetic radiation associated with lightning stepped-leaders *Geophys. Res. Lett.* **28** 2141

Moss G D, Pasko V P, Liu N and Veronis G 2006 Monte Carlo model for analysis of thermal runaway electrons in streamer tips in transient luminous events and streamer zones of lightning leaders *J. Geophys. Res.* **111** 2307

Nguyen C V, van Deursen A P J and Ebert U 2008 Multiple x-ray bursts from long discharges in air *J. Phys. D: Appl. Phys.* **41** 234012

Nguyen C V, van Deursen A P J, van Heesch E J M, Winands G J J and Pemen A J M 2010 X-ray emission in streamer-corona plasma *J. Phys. D: Appl. Phys.* **43** 025202

Rahman M, Cooray V, Ahmad N A, Nyberg J, Rakov V A and Sharma S 2008 X-rays from 80-cm long sparks in air *Geophys. Res. Lett.* **35** L06805

Roussel-Dupré R A, Gurevich A V, Tunnell T and Milikh G M 1994 Kinetic theory of runaway air breakdown *Phys. Rev.* E **49** 2257

Roussel-Dupré R, Colman J J, Symbalisty E, Sentman D and Pasko V P 2008 Physical processes related to discharges in planetary atmospheres *Space Sci. Rev.* **137** 51

Santos J P, Parente F and Kim Y-K 2003 Cross sections for K-shell ionization of atoms by electron impact *J. Phys. B: At. Mol. Opt. Phys.* **36** 4211

Scofield J H 1978 K- and L-shell ionization of atoms by relativistic electrons *Phys. Rev.* A **18** 963

Smith D M, Lopez L I, Lin R P and Barrington-Leigh C P 2005 Terrestrial gamma-ray flashes observed up to 20 MeV *Science* **307** 1085